**HEFAT2010**
**7th International Conference on Heat Transfer, Fluid Mechanics and Thermodynamics**
**19-21 July 2010**
**Antalya, Turkey**

# NUMERICAL STUDY OF OPTIMUM PIN-FIN HEAT SINK WITH AIR IMPINGING COOLING BY USING TAGUCHI METHOD

S.W. Hsiao*[1], Y.T. Yang[2], H.T. Hsu[2], H.S. Peng[3]
*Author for correspondence
[1]Department of Industrial Design
National Cheng Kung University,
Tainan, 701,
Taiwan, R.O.C.
E-mail: swhsiao@mail.ncku.edu.tw
[2]Department of Mechanical Engineering,
National Cheng Kung University,
[3]Department of Aeronautics and Astronautics
National Cheng Kung University

## ABSTRACT

This study presents the numerical simulation of optimum pin-fin heat sink with air impinging cooling by using Taguchi method. $L_9$ ($3^4$) orthogonal array is selected as a plan for the four design-parameters with three levels. The governing equations are discretized by using control-volume-based-finite-difference method with power-law scheme on an orthogonal non-uniform staggered grid. The coupling of the velocity and the pressure terms of momentum equations are solved by SIMPLEC algorithm. The $k-\varepsilon$ two-equations turbulence model is employed to describe the turbulent structure and behavior.

The parameters studied include fin height $H$ (35 mm – 45 mm), inter-fin spacing $a$ (2 mm - 6.4 mm), inter-fin spacing $b$ (2 mm - 6.4 mm), inter-fin spacing $c$ (2 mm - 6.4 mm), and Reynolds number ($\mathrm{Re} = 10000$ - 25000). The objective of this study is to examine the effects of the fin spacings and fin height on the thermal resistance and then find the optimum group by using Taguchi method. It's found that the fin spacings from center to edge of the heat sink should be gradually extended, and the fin's height is the longer the better. Then, the optimum group is $H_3a_1b_2c_3$. In addition, the effects of parameters are ranked by importance as $a$, $H$, $c$, and $b$.

## INTRODUCTION

The rapid progress of electronic technology causes the sizes of electronic components to shrink and the heat flux per unit area increased dramatically over the past decade. Thus, the efficient cooling and maintaining the die at a reasonable operating temperature have played an important role in ensuring a reliable operation of electronic components.

A number of research scholars have examined the thermal and hydraulic characteristics of various heat sinks extensively. Ledezma et al. [1] performed an experimental, numerical and theoretical study of the heat transfer on a pin-finned plate. They demonstrated the optimization principle experimentally by comparing several spacing designs in the same air stream in a wind tunnel. The correlation equations for optimal fin-to-fin spacing and the maximum thermal conductance were also developed. Brignoni and Garimella [2] demonstrated the experimental optimization of confined impinging air jets used in conjunction with a pin-fin heat sink. Enhancement factors for the heat sink relative to a bare surface were evaluated, and were in the range of 2.8 ~ 9.7, with the largest value being obtained for the largest single nozzle. Both the average heat transfer coefficients and the thermal resistance were expressed for the heat sink as a function of a Reynolds number, an air flow rate, a pumping power, and a pressure drop, to assist in optimizing the jet impingement configuration for given design constraints. Maveety and Hendricks [3] showed the performance study of pin-fin heat sinks with impingement cooling which considered the effects of geometry, nozzle-to-heat sink vertical placement, material, and Reynolds number. The results revealed that there is an optimal nozzle-to-sink height and Reynolds number for which the heat dissipation is maximized. The best performance occurred when the dimensionless impingement distance was between eight and twelve, and when the Reynolds number was between 40000 and 50000. The results also presented that due to the higher spreading resistance efficiency of the carbon composite material, it led to more uniform cooling of the heat sink. Moreover, the influence of the nozzle-to-heat sink vertical placement on the thermal performance was reduced as the Reynolds number increased. The comparisons between

computational and experimental results for the cooling performance from a pin-fin heat sink with an impinging air flow have been investigated by Maveety and Jung [4]. Furthermore, optimization studies were discussed to quantify the effects of changing the fin length and the fin cross-sectional area on the cooling performance. The numerical results illustrated a complex pressure gradients inside the fin array and a greater pressure gradient improved mixing and heat transfer. It also revealed that a complicated fluid motion with large pressure gradients generated vorticity, circulation and flow reversals. The enhancement of heat transfer from a discrete heat source in a confined air jet impingement was experimentally studied by El-Sheikh and Garimella [5]. A variety of pin-fin heat sinks were mounted on the heat source and the resulting enhancement discussed. Relative to an unpinned heat sink, the heat transfer from the pinned ones was improved by 2.4 to 9.2 times. Due to the introduction of the heat sinks, the enhancement factors relative to the bare heat source varied from 7.5 to 72. Results for the average heat transfer coefficient were correlated as a function of the Reynolds number, fluid properties and geometric parameters of the heat sinks. The thermal performance of pin-fin heat sinks with air impingement cooling was performed numerically and experimentally by Li and Chen [6]. The effects of the fin geometry and the Reynolds number on the heat transfer of the heat sinks were discussed, too. Sathe and Sammakia [7] have presented a study of a new and unique high-performance air-cooled impingement heat sink. The comparisons between numerical simulation and experimental data of the heat sink performance have been conducted. The effects of the fin thickness, inter-fin gap, nozzle width, and fin shape on the heat transfer and pressure drop have been studied. The study showed that the pressure drop can be decreased by cutting the fins in the central impingement zone without sacrificing heat transfer rates. The thermal performance of a pin-fin heat sink was studied theoretically and experimentally by Kobus and Oshio [8]. And a theoretical model was formulated that has the capability of predicting the influence of various geometrical, thermal, and flow parameters on the effective thermal resistance of the heat sink. Besides, the predictive capability of the theoretical model was verified by comparing with experimental data and was shown to be exceptionally good over the range of parameters. A theoretical and experimental was carried out investigating the influence of thermal radiation on the thermal performance of a pin fin array heat sink by Kobus and Oshio [9]. A theoretical thermal radiation model, which was validated by experimental data, was developed for predicting the effective thermal resistance of a fin array heat sink. The thermal and hydraulic behavior due to jet impingement on pin fin heat sinks was experimentally investigated by Issa and Ortega [10]. This study showed that the pressure loss coefficient increased with increasing pin density and pin diameter, and decreased with increasing pin height and clearance ratio. Moreover, the overall base-to-ambient thermal resistance decreased with increasing Reynolds number, pin density and pin diameter. Duan and Muzychka [11] performed the experimental investigation of the thermal performance with four heat sinks of various impingement inlet widths, fin spacings, fin heights and airflow velocities. They developed a heat transfer model to predict the thermal performance of impingement air cooled plate fin heat sinks for design purposes. Ledezma and Bejan [12] performed the experimental and numerical study of heat sinks with sloped plate fins. The study of pin fin heat sink with un-uniform fin height design with a confined impingement cooling was performed by Yang and Peng [13]. The results presented that an adequate un-uniform fin height design could decrease the junction temperature and increase the enhancement of the thermal performance simultaneously. This study discussed the thermal performance on the orientation of the fin array and the tilting of the crests of the plate fins.

## NOMENCLATURE

| | | |
|---|---|---|
| $a$ | [mm] | Inter-fin spacing |
| $b$ | [mm] | Inter-fin spacing |
| $c$ | [mm] | Inter-fin spacing |
| $C_1$ | [-] | Closure coefficients for the turbulence equation |
| $C_2$ | [-] | Closure coefficients for the turbulence equation |
| $COE$ | [-] | Coefficient of enhancement ( $= Nu/Nu_{origin}$ ) |
| $d$ | [m] | Diameter of nozzle |
| $h$ | [W/m$^2$K] | Convective heat transfer coefficient |
| $H$ | [mm] | Fin height |
| $k$ | [m$^2$/s$^2$] | Turbulent kinetic energy |
| $k_a$ | [W/mK] | Thermal conductivity for air |
| $k_s$ | [W/mK] | Thermal conductivity for solid |
| $Nu$ | [-] | Nusselt number ( $= h \cdot d/k_a$ ) |
| $P$ | [Pa] | Pressure |
| $q''$ | [W/m$^2$] | Wall heat flux |
| $Q$ | [W] | Heat addition |
| Re | [-] | Reynolds number ( $= \lvert V_{in} \rvert \cdot d/\nu$ ) |
| $R_{th}$ | [K/W] | Thermal resistance |
| $T$ | [K] | Temperature |
| $u$ | [m/s] | Velocity component |
| $W_{in}$ | [m/s] | Inlet velocity |
| $x$ | [m] | Cartesian coordinate |
| $y_i$ | [-] | Performance value of the $i$th experimental |

Greek symbols

| | | |
|---|---|---|
| $\varepsilon$ | [m$^2$/s$^2$] | Dissipation rate of turbulent kinetic energy |
| $\mu$ | [Ns/m$^2$] | Dynamic viscosity |
| $\nu$ | [m$^2$/s] | Kinematic viscosity |
| $\rho$ | [kg/m$^3$] | Density |
| $\sigma$ | [-] | Prandtl number |

Superscripts

| | | |
|---|---|---|
| $\bar{}$ | [-] | Time-averaged quantity |

Subscripts

| | | |
|---|---|---|
| $ave$ | [-] | Average |
| $i$ , $j$ | [-] | Indices |
| $in$ | [-] | Inlet |
| $k$ | [-] | Turbulent kinetic energy |
| $s$ | [-] | Solid |
| $t$ | [-] | Turbulent |
| $\varepsilon$ | [-] | Dissipation rate of turbulent kinetic energy |

## MATHEMATICAL MODEL AND NUMBERICAL METHOD

*Geometrical configuration and boundary conditions*

The schematic diagram of the geometry and the computational domain is shown in Fig. 1. The dimensions of the

computational domain were based on the work by Li and Chen [6]. Taking advantage of the symmetry, the numerical simulations have been performed by considering only a one-quarter model of the physical domain. The boundary conditions for this problem are stated as follows: At the flow inlet, the air was uniformly induced downward with a constant temperature.

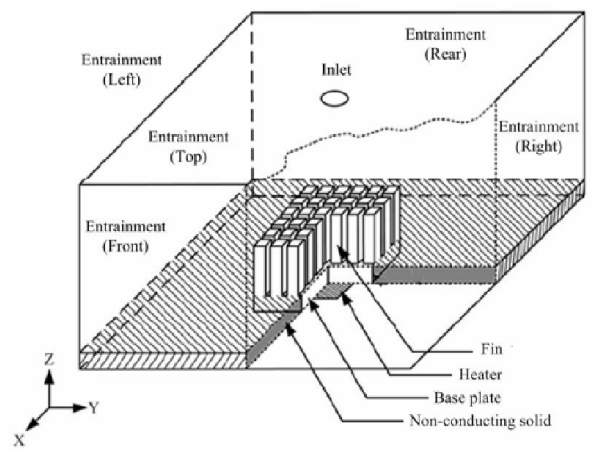


Fig. 1 Physical domain

The entrainment boundary conditions are used at the outlet. No slip conditions with thermally insulated are provided on all the other walls. At the bottom of the heat sink, a uniform constant heat flux is applied on the heating area. The adiabatic thermal boundary conditions are utilized at the outer perimeter of the bottom of heat sink except for the heating area.

*Governing equations*

The turbulent three-dimensional Navier-Stokes and energy equations are solved numerically (using a finite difference scheme) combined with the continuity equation to simulate the thermal and turbulent flow fields. An eddy viscosity model is used to account for the effects of turbulence. The flow is assumed to be steady, incompressible, and three-dimensional. The buoyancy and radiation heat transfer effects are neglect. In addition, the thermophysical properties of the fluid are assumed to be constant. The three-dimensional governing equations of mass, momentum, turbulent kinetic energy, turbulent energy dissipation rate, and energy in the steady turbulent main flow using the standard $k-\varepsilon$ model are as follows:

(1) Continuity equation

$$\frac{\partial \rho \overline{u}_i}{\partial x_i} = 0 \tag{1}$$

(2) Momentum equation

$$\rho \overline{u}_j \frac{\partial \overline{u}_i}{\partial x_j} = -\frac{\partial \overline{p}}{\partial x_i} + \frac{\partial}{\partial x_j}\left[ (\mu + \mu_t)\left( \frac{\partial \overline{u}_i}{\partial x_j} + \frac{\partial \overline{u}_j}{\partial x_i} \right) \right] \tag{2}$$

(3) Energy equation

$$\rho \overline{u}_j \frac{\partial \overline{T}}{\partial x_j} = \frac{\partial}{\partial x_j}\left[ \left( \frac{\mu_l}{\sigma_l} + \frac{\mu_t}{\sigma_T} \right) \frac{\partial \overline{T}}{\partial x_j} \right] \tag{3}$$

(4) Solid energy equation

$$\frac{\partial}{\partial x_i}\left( k_s \frac{\partial T}{\partial x_i} \right) = 0 \tag{4}$$

(5) Transport equation for $k$

$$\rho \overline{u}_j \frac{\partial k}{\partial x_j} = \frac{\partial}{\partial x_j}\left[ \left( \mu + \frac{\mu_t}{\sigma_k} \right) \frac{\partial k}{\partial x_j} \right] + \mu_t \left( \frac{\partial \overline{u}_i}{\partial x_j} + \frac{\partial \overline{u}_j}{\partial x_i} \right) \frac{\partial \overline{u}_i}{\partial x_j} - \rho \varepsilon \tag{5}$$

(6) Transport equation for $\varepsilon$

$$\rho \overline{u}_j \frac{\partial \varepsilon}{\partial x_j} = \frac{\partial}{\partial x_j}\left[ \left( \mu + \frac{\mu_t}{\sigma_\varepsilon} \right) \frac{\partial \varepsilon}{\partial x_j} \right] + C_1 \mu_t \frac{\varepsilon}{k}\left( \frac{\partial \overline{u}_i}{\partial x_j} + \frac{\partial \overline{u}_j}{\partial x_i} \right) \frac{\partial \overline{u}_i}{\partial x_j} - C_2 \rho \frac{\varepsilon^2}{k} \tag{6}$$

*Data reduction*

The Reynolds number of the impinging jet is defined as

$$\mathrm{Re} = \frac{|W_{in}|\, d}{\nu} \tag{7}$$

where $d$ denotes the diameter of nozzle.

As far as evaluating the efficiency of heat dissipation, "thermal resistance" is often used to rate the performances of the heat sink. The thermal resistance of the heat sink, $R_{th}$, can be defined by

$$R_{th} = \frac{T_{ave} - T_{in}}{Q} \tag{8}$$

where $T_{ave}$ and $T_{in}$ are average temperature of the base of the heat sink and the temperature of the inlet fluid, respectively. $Q$ is the heating power applied on the base of heat sink.

The coefficient of enhancement (COE) is defined to quantify the improvement in heat transfer rates due to the different types of the heat sink fins. This is expressed as

$$COE = \frac{Nu_{new}}{Nu_{origin}} \tag{9}$$

where the average Nusselt number $Nu$ is calculated by

$$Nu = \frac{hd}{\mathrm{k_a}} \tag{10}$$

and the average convection heat transfer coefficient $h$ is calculated by

$$h = \frac{q''}{T_{base} - T_{in}} \tag{11}$$

*Numerical approach*

A non-uniform and staggered grid system was employed. A staggered grid arrangement is used in which the velocities are stored at a location on the control-volume faces. All other variables including pressure are calculated at the grid points. The numerical method used in the present study is base on the SIMPLEC algorithm [14]. Pressure and velocity correction schemes are implemented in the model algorithm to arrive at a converged solution when both the pressure and velocity satisfy the momentum and continuity equations. For non-linear problems, under-relaxation is employed to avoid divergence in the iterative solutions. The resulting sets of discretized equations for each variable are solved by the line-by-line procedure which is the combination of the Tri-Diagonal Matrix Algorithm (TDMA) and the Gauss-Seidal iteration technique. The solution is considered to be converged when the

normalized residual of the algebraic equation is less than a prescribed value of $10^{-3}$.

*Taguchi method*

In the present study, all the parameters influence the thermal resistance and pressure drop have not been investigated in detail, because it requires a large number of simulations and time taken. Taguchi method developed by Genichi Taguchi is a useful method for systematically optimized designs. The number of simulations required for a whole analysis in the case of four three-level parameters can be reduced from 81 ($3^4$) to 9. The $L_9(3^4)$ orthogonal array can be adopted for further analysis of sensitivity of each parameter. Table 1 and Table 2 list the values of four factors and three levels and nine cases for $L_9(3^4)$ orthogonal array. The parameters affecting thermal resistance, namely fin height $H$, inter-fin spacing $a$, inter-fin spacing $b$, inter-fin spacing $c$ (denote in Fig. 2) are inserted in columns A, B, C, D. The purpose is to obtain the minimum thermal resistance. The performance statistics were chosen as the optimization criterion. It was used for "the smaller the better" situations, evaluated using the following equation:

$$S/N = -10\log\left(\frac{\sum_{i=1}^{n} y_i^2}{n}\right) = -\log\left(\bar{y}^2 + S^2\right) \quad (12)$$

Table 1 $L_9(3^4)$ orthogonal array of the Taguchi method

| Case no. | Parameters and their levels | | | |
|---|---|---|---|---|
| | A | B | C | D |
| 1 | 1 | 1 | 1 | 1 |
| 2 | 1 | 2 | 2 | 2 |
| 3 | 1 | 3 | 3 | 3 |
| 4 | 2 | 1 | 2 | 3 |
| 5 | 2 | 2 | 3 | 1 |
| 6 | 2 | 3 | 1 | 2 |
| 7 | 3 | 1 | 3 | 2 |
| 8 | 3 | 2 | 1 | 3 |
| 9 | 3 | 3 | 2 | 1 |

Table 2 Factors used in the Taguchi method

| Parameters | Levels | | |
|---|---|---|---|
| | 1 | 2 | 3 |
| A: Fin height ($H$) (mm) | 35 | 40 | 45 |
| B: Inter-fin spacing ($a$) (mm) | 2 | 4.2 | 6.4 |
| C: Inter-fin spacing ($b$) (mm) | 2 | 4.2 | 6.4 |
| D: Inter-fin spacing ($c$) (mm) | 2 | 4.2 | 6.4 |

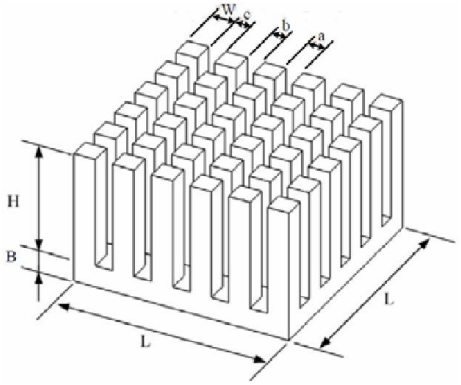


Fig. 2 Denotations of the pin fin heat sink

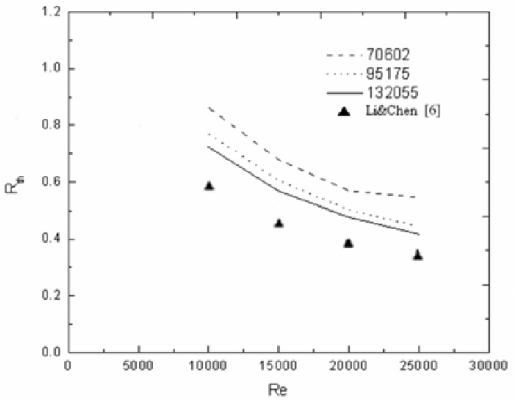


Fig. 3 Grid Refinement

## RESULTS AND DISCUSSION

The dimensions of the heat sink in this study were based on the work by Li and Chen [6]. Both of the length and width of the base of the heat sink are 80 mm. The area of the heater is 40 mm × 40 mm, which is in the center of the heat sink. And the heating area is heated with heating power 20W.

The parameters used in the grid refinement test were based on the uniform inter-fin spacing design and $H$ = 40 mm. A total number of meshes, 70602, 95175 and 132055 were employed to assess the grid independence. As shown in Fig. 3, the results of the grid sensitivity study showed that the simulations based on the 95175 meshes provide satisfactory numerical accuracy.

From Table 3 and Fig. 4, it can be seen that the most effective parameters on the thermal resistance are found as follows: the inter-fin spacing ($a$), the fin height ($H$), the inter-fin spacing ($c$), the inter-fin spacing ($b$). The thermal resistance decreases by increasing the fin height. Increasing the fin height enlarges the heat transfer area of the heat sink, which enhances the heat transfer rate. Hence, the thermal performance improved. The thermal resistance increases by increasing the inter-fin spacing $a$. The thermal resistance decreases when the inter-fin spacing $b$ changes from 2 mm to 4.2 mm, and then increases when inter-fin spacing $b$ changes from 4.2 mm to 6.4 mm. And the effect of inter-fin spacing $c$ is contrary to inter-fin spacing $a$. The thermal resistance decreases when increases the inter-fin spacing $c$. It is important to enlarge the heat transfer area for the efficient heat dissipation in the central

region of the heat sink. Therefore, the inter-fin spacing $a$ should be decreased in the center of the heat sink to increase the heat transfer area in the central region. And the momentum of working fluid is weak around the rim of the heat sink. Hence, the inter-fin spacing $c$ should be increase to reduce the flow resistance and allow more working fluid flow out.

Table 3 The S/N values and effects of each parameter

| | A | B | C | D |
|---|---|---|---|---|
| Level-1 | 4.243146 | 5.185925 | 4.577446 | 4.264682 |
| Level-2 | 4.606064 | 5.014490 | 5.020508 | 4.706879 |
| Level-3 | 5.159856 | 3.808650 | 4.411112 | 5.037505 |
| Effect | 0.916709 | 1.377276 | 0.609395 | 0.772823 |
| Rank | 2 | 1 | 4 | 3 |
| Best | 5.159856 | 5.185925 | 5.020508 | 5.037505 |

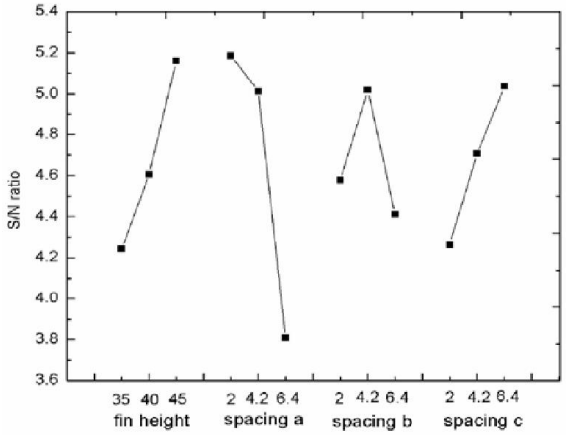


Fig. 4 The effect of each parameter on the thermal resistance ( Re = 15000)

Fig. 5 shows the simulations of Nusselt number of three heat sinks as a function of Reynolds number. From Fig. 5, it is seen that increasing the Reynolds number increases the Nusselt number. However, the increment of the Nusselt number decreases gradually as the Reynolds number increases. The figure also shows the comparison of Nusselt number between original and optimal designs. The result of optimum condition on the Nusselt number is much higher than the original designs.

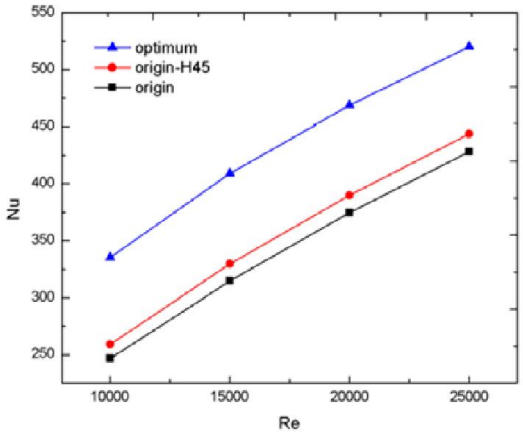


Fig. 5 Simulations of Nusselt number of three heat sinks as a function of Reynolds number

The effects of the Reynolds number and the fin design (better than the original design) on COE is shown in Fig. 6. Although the fin height of case 9 is higher than case 2 and 4, the COE of case 9 is lower than those. Because the flow penetration into the heat sink becomes weaker due to the increased flow resistance. Hence, the inter-fin spacing should be designed appropriate for more working fluid flow into the heat sink. Moreover, it can be seen that COE decreases when the Reynolds number increases. The enhancement of the heat transfer by increasing the Reynolds number may have a limitation.

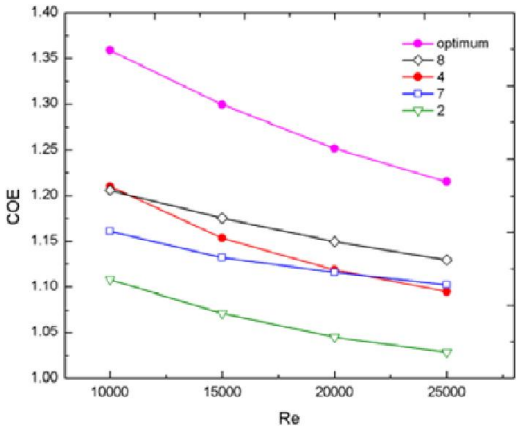


Fig. 6 Effects of the Reynolds number and the fin design (better than the original design) on COE

## CONCLUSIONS

The present study provides valuable information on the pin-fin heat sink with air impinging cooling by numerical simulation with Taguchi method. The parameters affecting thermal performance have been systematically investigated by using $L_9$ ($3^4$) orthogonal array. The governing equations are discretized by using control-volume-based-finite-difference method with power-law scheme on an orthogonal non-uniform staggered grid. The coupling of the velocity and the pressure terms of momentum equations are solved by SIMPLEC algorithm. The $k-\varepsilon$ two-equations turbulence model is employed to describe the turbulent structure and behavior. The parameters studied include fin height $H$ (35 mm, 40 mm, 45 mm), inter-fin spacing $a$ (2 mm, 4.2 mm, 6.4 mm), inter-fin spacing $b$ (2 mm, 4.2 mm, 6.4 mm), inter-fin spacing $c$ (2 mm, 4.2 mm, 6.4 mm). The results of the present study are described as follows.

(1) The optimum group is $H_3a_1b_2c_3$, i.e. $H$ = 45 mm, $a$ = 2 mm, $b$ = 4.2 mm, $c$ = 6.4 mm.

(2) The effects of parameters are ranked by importance as $a$, $H$, $c$, and $b$.

(3) It is found that an adequate arrangement of inter-fin spacing could increase the Nusselt number and COE. The increments of the Nusselt number and COE decrease gradually as the Reynolds number increases. At high Reynolds number, the effects of geometries are decayed.

## ACKNOWLEDGEMENTS

The support of the National Science Council (NSC) of Taiwan under contract No. NSC 96-2221-E-006-161-MY2 is gratefully acknowledged. The authors also want to thank the National Center for High-Performance Computing (NCHC) for computer time and facilities.

## REFERENCES

[1] Ledezma G., Morega A.M., and Bejan A., Optimal Spacing between Pin Fins with Impinging Flow, *Journal of Heat Transfer*, Vol. 118, 1996, p.p. 570-577

[2] Brignoni L.A., and Garimella S.V., Experimental optimization of confined air jet impingement on a pin fin heat sink, *IEEE Transactions on Components and Packaging Technologies*, Vol. 22, no. 3, 1999, p.p. 399-404

[3] Maveety J.G., and Hendricks J.F., A heat sink performance study considering material, geometry, Reynolds number with air impingement, *Journal of Electronic Packaging*, Vol. 121, 1999, p.p. 156-161

[4] Maveety J.G., and Jung H.H., Design of an optimal pin-fin heat sink with air impingement cooling, *International Communications in Heat and Mass Transfer*, Vol. 27, no. 2, 2000, p.p. 229-240

[5] El-Sheikh H.A., and Garimella S.V., Enhancement of air jet impinging heat transfer using pin-fin heat sinks, *IEEE Transactions on Components and Packaging Technologies*, Vol. 23, no. 2, 2000, p.p. 300-308

[6] Li H.Y., and Chen K.Y., Thermal-fluid characteristics of pin-fin heat sinks cooled by impinging jet, *Journal of Enhanced Heat Transfer*, Vol.12, no. 2, 2005, p.p. 189-201

[7] Sathe S.B., and Sammakia B.G., An analytical study of the optimized performance of an impingement heat sink, *Journal of Electronic Packaging*, Vol.126, 2004, p.p. 528-534

[8] Kobus C.J., and Oshio T., Development of a theoretical model for predicting the thermal performance characteristics of a vertical pin-fin array heat sink under combined forced and natural convection, *International Journal of Heat and Mass Transfer*, Vol.48, 2005, p.p. 1053-1063

[9] Kobus C.J., and Oshio T., Predicting the thermal performance characteristics of staggered vertical pin fin array heat sinks under combined mode radiation and mixed convection with impinging flow, *International Journal of Heat and Mass Transfer*, Vol. 48, 2005, p.p. 2684-2696

[10] Issa J.S., and Ortega A., Experimental Measurements of the Flow and Heat Transfer of a Square Jet Impinging on an Array of Square Pin Fins, *Journal of Electronic Packaging*, Vol. 128, 2006, p.p. 61-70

[11] Duan Z., and Muzychka Y.S., Experimental investigation of heat transfer in impingement air cooled plate fin heat sinks, *Journal of Electronic Packaging*, Vol. 128, 2006, p.p. 412-418

[12] Ledezma G., and Bejan A., Heat sinks with sloped plate fins in natural and forced convection, *International Journal of Heat and Mass Transfer*, Vol. 39, no. 9, 1996, p.p. 1773-1783

[13] Yang, Y.T., and Peng, H.S., Numerical study of pin-fin heat sink with un-uniform fin height design, *International Journal of Heat and Mass Transfer*, Vol. 51, no. 19-20, 2008, p.p. 4788-4796

[14] Doormaal J.P. van, and Raithby F.D., Enhancements of the SIMPLE method for predicting incompressible fluid flows, *Numerical Heat Transfer*, Vol. 7, 1984, p.p. 147-163